

Collapse of the $4f$ orbital for Xe-like ions

K. T. Cheng

Argonne National Laboratory, Argonne, Illinois 60439

C. Froese Fischer

Computer Science Department, Vanderbilt University, Nashville, Tennessee 37235

(Received 27 September 1982; revised manuscript received 23 May 1983)

The effect of $4f$ orbital collapse on the spectra of Xe-like ions in the region of $4d \rightarrow nf, \epsilon f$ excitations is studied with the use of a term-dependent Hartree-Fock technique. We find that the collapse of the $4f$ orbital is strongly term dependent, and that the appearance of intense absorption lines in the observed Ba^{2+} spectrum is due to the partial collapse of the $4f$ orbital in the $4d \rightarrow f^1P$ channel. We also show that after the $4f$ orbital is completely collapsed for high degrees of ionization along the isoelectronic sequence, the bulk of absorption oscillator strengths is concentrated at the $4d^9 4f^1P$ level so that the only strong line in the spectrum is again the $4d \rightarrow 4f^1P$ transition.

I. INTRODUCTION

The formation of neutral rare earth elements is due to the filling of the $4f$ shell in the rare-earth region of the periodic table. Goepfert Mayer¹ first pointed out that the properties of these atoms depend on the sudden decrease in energy and size of the $4f$ wave function at the beginning of this group of elements. This is usually called the collapse of the $4f$ orbital which arises because of specific features of the effective potential for f electrons. The effective potential is determined by the atomic central potential $V(r)$ and the centrifugal term $l(l+1)/2r^2$ as $V_{\text{eff}}(r) = V(r) + l(l+1)/2r^2$ (atomic units are used throughout this paper). For f electrons of heavy atoms, it consists of two wells separated by a potential barrier. The outer well is dominated by the long-range Coulomb potential and behaves asymptotically as $-1/r$ for neutral atoms. It is broad and shallow and can support an infinite Rydberg series of nf bound states. The inner well, on the other hand, is much narrower and deepens with increasing nuclear charge Z . For lighter atoms, it is not deep enough to support any bound state and all nf wave functions reside in the outer well. The first bound state of the inner well appears near $Z=58$, leading to the sudden collapse of the $4f$ wave functions from the outer into the inner well.

Through the years, there have been many studies on the absorption spectra of atoms or ions with $Z=54-70$ in the region of $4d \rightarrow nf, \epsilon f$ excitations.²⁻⁴ These spectra are characterized by strong absorption peaks above the $4d$ ionization limits, with widths ranging from 15-70 eV, and weak absorption lines in the discrete excitation region. For lighter elements in this group, such as neutral Xe, the potential barrier keeps low-energy f orbitals outside the region where the $4d$ wave functions are confined. As a result, the peaks in the observed spectra arise from delayed onsets of $4d \rightarrow f$ transitions which become intense only at energies high enough for the final state f electrons to surmount the potential barrier.⁵ For heavier elements ($Z \geq 56$), the explanation of the observed spectra is more complicated. Since the inner well of the effective potential is now deep enough to hold a "collapsed" $4f$ orbital,

the overlap between the $4d$ and $4f$ orbitals should increase dramatically, while those between the $4d$ and higher nf orbitals remain small because the potential barrier still prevents low-energy f wave functions from entering the inner region. Thus the spectra should show delayed onsets of photoionizations, but in addition, there should be strong absorption lines from the $4d \rightarrow 4f$ transitions and these are not observed. The absence of intense absorption lines in the observed spectra is generally explained as due mainly to the raising of the $4d \rightarrow 4f^1P$ discrete level into the f continuum as a result of strong exchange effects.⁶ The giant resonancelike peaks above the ionization limits in the observed spectra are interpreted as evidence of a strong interaction between $4f^1P$ and the continuum. However, consistent applications of such interpretations are difficult and often confusing.

The spectrum of Ba^{2+} is a case at hand. Using a two-step laser excitation technique, Lucatorto *et al.*⁷ measured the absorption spectra of Ba, Ba^+ , and Ba^{2+} in the region of $4d \rightarrow f$ excitations. They found that the spectra of Ba and Ba^+ show typical strong absorption peaks above the $4d$ ionization limits and weak resonance lines below them. The spectrum of Ba^{2+} , on the other hand, is entirely different. The absorption cross section now starts from a sizeable value (~ 30 Mb) at the $4d$ threshold and decreases monotonically afterwards (up to about 160 eV). At the same time, several strong resonance lines appear in the discrete excitation region. The sudden change in the spectra from Ba^+ to Ba^{2+} is attributed to the collapse of the $4f$ orbital, but the interpretation of the Ba^{2+} spectrum presents difficulties.

Even after the $4f$ orbital is collapsed, it is expected that the potential barrier should still prevent higher nf wave functions from entering the inner well, which cannot support any more bound states. Accordingly, there should be either only one strong resonance line from the $4d \rightarrow 4f^1P$ transition or none at all if the $4f^1P$ level is raised into the continuum. This prompted Lucatorto *et al.* to suggest that the $4f$ orbital is only partially collapsed in Ba^{2+} , a view supported by their configuration-average Hartree-Fock (HF) results, which showed that in Ba^{2+} the ex-

change interaction is not strong enough to push the $4f^1P$ level all the way into the continuum. This view is supported also, to some extent, by Connerade and Mansfield⁸ who suggested that the $4f^1P$ level is suffering from a "collapse of the second kind," and that the nf wave functions are hybridized (i.e., with comparable amplitude in both the inner and outer wells), resulting in strong absorptions from $4d \rightarrow nf^1P$ transitions. However, contrary to the findings of Lucatorto *et al.*, their configuration-interaction (CI) results showed that the $4f^1P$ level was imbedded in the continuum,⁹ and that the observed resonance lines actually came from $4d \rightarrow 5f, 6f, \dots^1P$ transitions.

Apart from the obvious discrepancy about the location of the $4f^1P$ level, there are other puzzling questions: For example, what causes the strong hybridization of nf wave functions in Ba^{2+} ? Are the identifications of the resonance lines correct? More generally, what is the nature of partial orbital collapse, or collapse of the second kind, and how are they related to the usual collapse phenomenon? Even though a recent time-dependent local-density approximation (TDLDA) calculation by Nuroh *et al.*¹⁰ successfully reproduced the dominant features of the absorption spectra for Ba, Ba^+ , and Ba^{2+} , these questions remain unanswered.

In this work, we present an interpretation of the Ba^{2+} spectrum from a term-dependent HF point of view.¹¹ Specifically, we study the $4d^9nf^1P$, 3P , and 3D levels for Xe-like ions. By studying the isoelectronic sequence, where these ions have the same electronic configuration, we can gain important insight into the collapse phenomenon from the systematic trends of these levels. In particular, we find that orbital collapse and partial orbital collapse are closely related to shape resonance effects in the continuum, and that the hybridization of nf wave functions is due to resonant enhancement of their amplitudes in the inner well regions. In the following, we shall begin by reexamining the causes of orbital collapse, and the possible consequences. We shall then present and discuss results of our calculations.

II. $4f$ ORBITAL COLLAPSE

In her discussion of the collapse phenomenon in neutral atoms, Goepfert Mayer¹ used a model where the inner and the outer potential wells for f electrons are divided by an infinite barrier. In such a model, the spectrum consists of two independent sets of levels, and the hydrogenlike spectrum of the outer well is unaffected by the presence of the inner well. For small Z , the first eigenstate of the inner well is much higher than the ionization limit. As Z increases, the inner well deepens and its first level eventually sinks below the entire Rydberg series of the outer well. This happens near $Z=58$ and leads to the sudden collapse of the $4f$ orbital from the outer into the inner well. As the inner well is narrow, its levels are widely spaced. Thus the collapse of the $5f$ orbital does not happen until $Z \simeq 90$, when the second level of the inner well also sinks below all the levels of the outer well.

We thus see that orbital collapse is caused by the lowering of the spectrum of the inner well relative to that of the

outer one. With an infinite barrier between the two wells, only the orderings of the levels are affected in the process. With a finite potential barrier, however, these two sets of levels interact with each other. The first sign of this interaction comes when the lowest level of the inner well gets below the potential barrier. There, it becomes a shape resonance and can "autoionize" into the continuum of the outer well by tunneling out of the potential barrier. A further increase in Z brings this level below the ionization limit, where it interacts with the entire nf series before sinking below all of them.

The existence of shape resonances in the effective potentials of the f electrons for Xe was shown by Manson and Cooper¹² in a Herman-Skillman potential calculation. Specifically, they found that the phase shifts of the continuum f orbitals go through step changes of π right above the $4d$ ionization limit. This is further verified by Cheng and Johnson¹³ in a recent relativistic random-phase approximation (RRPA) study of the photoionization of the $4d$ shells for Xe-like ions. There, the $4d \rightarrow f$ transitions are shown to be strongly term dependent. In particular, the shape resonances in the 3P and 3D channels are very sharp, while that in the 1P channel is much broader. Furthermore, these shape resonances appear to move below the $4d$ ionization limit starting from Cs^+ .

Even after the first eigenstate of the inner well is lowered into the discrete excitation region, its interaction with the nf levels of the outer well can still be studied as a resonance phenomenon. Indeed, according to quantum-defect theory,¹⁴ the phase shifts δ of the continuum states are related to the quantum defects μ of the bound states as $\delta = \pi\mu$. The quantum defect is defined by the Rydberg formula

$$E_n = -Z_c^2/2\nu^2 = -Z_c^2/2(n - \mu)^2. \quad (1)$$

Here E_n is the energy of the bound state relative to the ionization limit, Z_c is the effective core charge, n is the principal quantum number, and ν is the effective quantum number. Like the phase shifts of the continuum states which go through step changes of π in passing through shape resonances, the quantum defects of the discrete levels in the outer well should increase by one when an eigenstate of the inner well passes by. Equivalently, ν has to decrease by one, as $\nu = n - \mu$. In particular, since the eigenstate of the inner well has to sink below the entire Rydberg series for orbital collapse to take place, all the nf levels will be affected in the process. This is verified, for example, by Band *et al.*¹⁵ who used a configuration-average Dirac-Fock technique to show that the effective quantum numbers of the $6s^2nf$ and $6s^24f^6nf$ levels indeed decrease by 1 when Z changes from 56 to 57 and from 62 to 63, respectively.

The lowering of the inner well eigenstate into the discrete excitation region with increasing Z , as well as the relation between shape resonances and orbital collapse has been reviewed by Karaziya³ and will not be discussed further here. We should point out, however, that the model described here follows the traditional view of orbital collapse for neutral systems. In this paper we study collapse along an isoelectronic sequence instead, in which case not only does the inner well deepen as Z increases, but also the

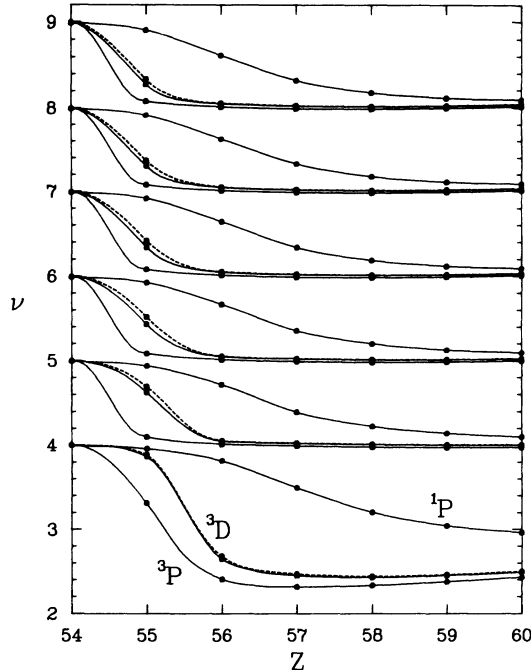


FIG. 1. Effective quantum numbers ν of the $4d^9nf$ 1P , 3P , and 3D states ($n=4-9$) for Xe-like ions as functions of the nuclear charge Z . Dashed curves are the configuration-average results.

outer well. Even so, the energy levels of the inner well sink so rapidly that the basic model of orbital collapse is unchanged. The implications of a deepening outer well will be discussed in Secs. III and IV.

III. RESULTS AND DISCUSSIONS

As a test of our model of orbital collapse and its application to the interpretation of the Ba^{2+} spectrum, we calculated effective quantum numbers of the $4d^9nf$ 1P , 3P , and 3D states ($n=4-9$) for Xe-like ions with a term-dependent HF technique.¹¹ Results are plotted as functions of Z in Fig. 1, along with those of the configuration-average $4d^9nf$ states. As one can see in Fig. 1, the effective quantum numbers of these states do decrease by 1 in the region considered. In particular, the effective quantum numbers of the $4d^94f$ states actually decrease by more than unity. This point will be discussed in more detail later.

In Fig. 1, one also notices that as Z increases, the effective quantum numbers of the triplet states go through step

changes of 1 much faster than those of the singlet state. This shows the strong term dependence of the collapse phenomenon, in accordance with similar findings in the RRPA studies of the $4d$ photoionization for Xe-like ions.¹³ An interesting observation here is that in Ba^{2+} , the $4f$ orbital is collapsed in the configuration-average state as well as in the 3P and 3D states, but is not quite collapsed in the 1P state. Similar term dependence in the collapse of the $4f$ orbital for neutral Ba atom has been pointed out before by Hansen *et al.*¹⁶

In Table I, we present HF results for the absorption oscillator strengths of the $4d^{10}S \rightarrow 4d^9nf$ 1P ($n=4-9$) transitions for Xe-like ions. The values reported are geometric means of the length and velocity form results. As one can see, these oscillator strengths are very small in neutral Xe, and increase rapidly with increasing Z . For Ba^{2+} , they are large enough to account for the strong resonance lines observed. But perhaps the most interesting feature here is that with further increase in Z the bulk of oscillator strengths gradually shifts to the $4d \rightarrow 4f$ 1P line so that for $Z \geq 58$ this single line completely dominates the spectrum.

The situation is clearly shown in Fig. 2, where we plot the theoretical absorption spectra for Xe-like ions. In Fig. 2, the absorption cross sections above the $4d$ thresholds are RRPA photoionization results of Cheng and Johnson.¹³ The rectangles below the $4d$ thresholds are effective oscillator strength distributions of this calculation. The area of each rectangle corresponds to the value of the discrete oscillator strength f_n given in Table I, and the height of each rectangle equals $f_n \nu_n^3 / Z_c^2$ [actually, since we are plotting cross sections σ in Mb, and since $\sigma(\text{Mb}) = 4.0336 df/d\epsilon$ (a.u.), the area and height of each rectangle should be $4.0336 f_n$ and $4.0336 f_n \nu_n^3 / Z_c^2$, respectively]. According to quantum-defect theory,¹⁴ the effective oscillator strength distribution varies slowly along the Rydberg series and continues smoothly onto the continuum spectrum. In Fig. 2, since the effective oscillator strength distributions and the ionization cross sections are calculated from different theoretical techniques, they do not match perfectly. Nevertheless, these spectra clearly show the gradual transfer of the oscillator strength from the continuum in Xe, to the collapsed $4f$ 1P state in higher Z ions.

The trend in the oscillator strengths demonstrates the effect of orbital collapse on the absorption spectrum. It can be understood as a resonance phenomenon. For neutral Xe, the shape resonance (inner well eigenstate) in the 1P channel leads to a giant peak in the spectrum above the $4d$ thresholds, with a width as broad as 70 eV.¹³ As this

TABLE I. Absorption oscillator strengths of the $4d^{10}S \rightarrow 4d^9nf$ 1P transitions for Xe-like ions.

n	Xe	Cs ⁺	Ba ²⁺	La ³⁺	Ce ⁴⁺	Pr ⁵⁺	Nd ⁶⁺
4	0.00009	0.020	0.586	4.315	7.167	8.090	8.049
5	0.00007	0.018	0.503	1.297	0.879	0.440	0.164
6	0.00005	0.014	0.328	0.591	0.327	0.114	0.018
7	0.00004	0.010	0.213	0.321	0.155	0.043	0.002
8			0.143	0.194	0.086	0.020	0.000
9			0.100	0.127	0.052	0.011	0.000

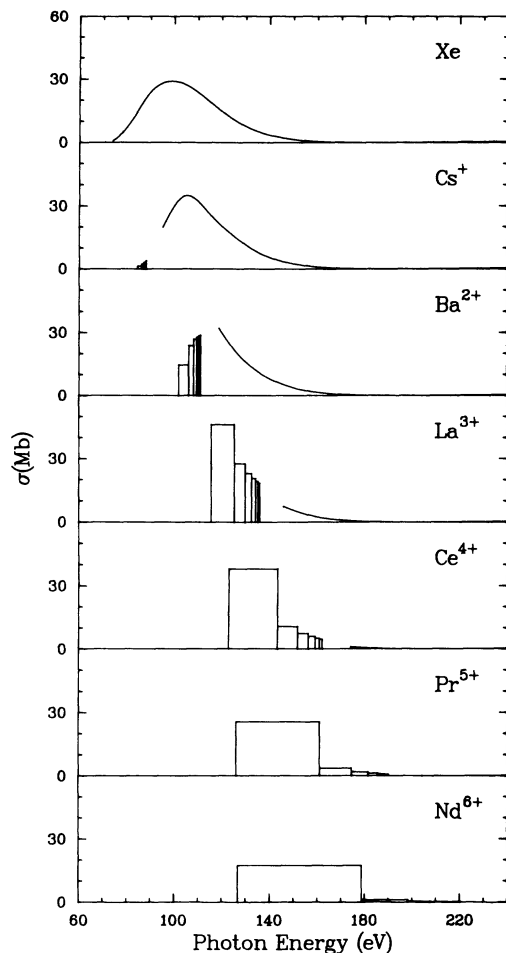


FIG. 2. Theoretical absorption spectra for Xe-like ions. Rectangles are effective oscillator strength distributions of this work for the $4d \rightarrow nf \ ^1P$ transitions ($n=4-9$). Continuum cross sections are RRPA results of Cheng and Johnson, Ref. 13.

shape resonance gradually moves below the ionization limits with increasing Z , interactions with nf levels are enhanced, resulting in the hybridization of nf wave functions and relatively large oscillator strengths for the discrete $4d \rightarrow nf \ ^1P$ transitions. (This is the situation between Ba^{2+} and Ce^{4+} .) Eventually, this shape resonance sinks below the entire nf Rydberg series and becomes a real bound state. Further increase in Z only widens the energy separations and diminishes the interaction between the collapsed $4f$ and higher nf states. As a result, the transition to the collapsed $4f \ ^1P$ level now carries most of the available oscillator strengths.

That orbital collapse is basically a resonance phenomenon can be further verified by analyzing the phase shift of the f wave function, which should go through step changes of π near a resonance. In Fig. 3, we plot the quantum defects μ_n of the $nf \ ^1P$ levels ($n=4-9$) as functions of photon energy, along with the RRPA eigenquantum defects $\mu(\epsilon) = \delta(\epsilon)/\pi$ for the $4d \rightarrow f \ ^1P$ channel ($\mu_{\alpha=3}$ in Ref. 13). As we have mentioned before, μ_n of a Rydberg series should continue smoothly into $\mu(\epsilon)$ of the continuum state. Again, μ_n and $\mu(\epsilon)$ do not match

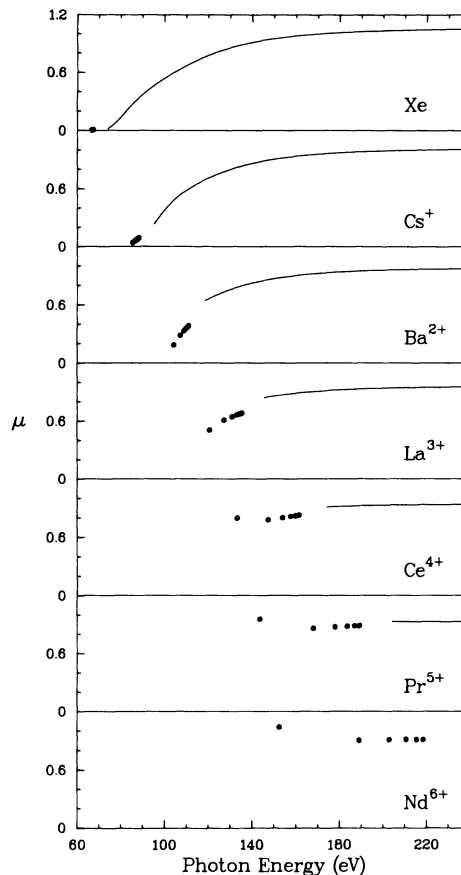


FIG. 3. Quantum-defect functions for Xe-like ions. Dots are HF quantum defects for the $nf \ ^1P$ state ($n=4-9$) calculated here. Solid lines are RRPA eigenquantum defects for the $4d \rightarrow f \ ^1P$ channel of Cheng and Johnson, Ref. 13.

perfectly here, but their energy variations for the first few members of the isoelectronic sequence do show the presence of shape resonances in the effective potential. Also it is obvious from Figs. 2 and 3 that the inner well eigenstate becomes the lowest $4f$ state in La^{3+} . As the collapsed $4f$ state does not belong to the Rydberg series of the outer well, its quantum defect starts to deviate from those of higher nf levels. In particular, the increasing isolation of the collapsed $4f$ state along the isoelectronic sequence leads to diminishing resonance effect on higher nf states and hence to slower energy variations in μ_n . This is most obvious in Fig. 3, starting from Ce^{4+} .

Based on our results, we can now present a clear description of orbital collapse and its effect on the Ba^{2+} spectrum. Ordinarily, orbital collapse happens so abruptly that the whole process can be completed with an increase in Z of less than one.¹⁵ Along the Xe isoelectronic sequence, however, it is obvious from Figs. 1-3 that the collapse in the 1P channel is very slow and covers several ions. This gives us a chance to observe the transition effect of partial orbital collapse, which happens when the inner well eigenstate is lowered into the discrete excitation region but is not yet below the entire Rydberg series. As the inner well eigenstate is close to the nf levels during partial orbital collapse, the amplitudes of nf wave func-

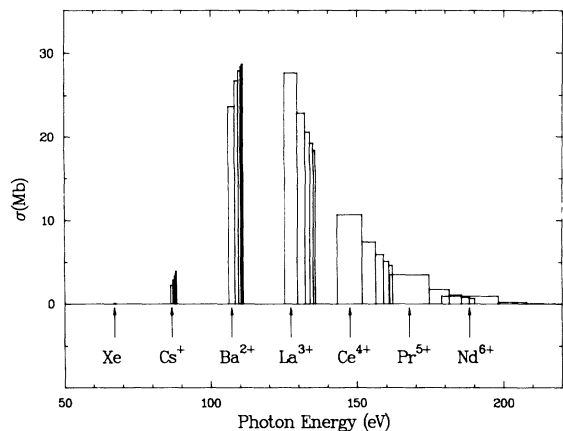


FIG. 4. Effective oscillator strength distributions for the $4d \rightarrow nf \ ^1P$ transitions ($n=5-9$) for Xe-like ions. Arrows are pointing at the centers of the $5f \ ^1P$ lines.

tions in the inner region are resonantly enhanced. An example of this “hybridization” of nf wave functions has already been given by Band *et al.*¹⁵ who showed that the probabilities of finding nf electrons in the inner region could go up by three orders of magnitudes in passing through the inner well resonance with increasing Z . Further discussions of hybrid wave functions can be found in Ref. 2.

Because of the hybridization of the nf wave functions, transitions to the $nf \ ^1P$ states are also resonantly enhanced. The effect is clearly shown in Fig. 2, especially between Ba^{2+} and Ce^{4+} . In Figs. 2 and 3, one also notices that, as a function of photon energy, the center of the inner well resonance (which becomes the $4f \ ^1P$ state after the collapse) really does not move too much along the isoelectronic sequence. Thus instead of the inner well resonance being lowered into the discrete excitation region as Z increases, the situation can also be described as one in which the energy of the nf series is being increased to pass through this resonance. Based on the latter picture, we can further demonstrate the effect of partial orbital collapse on discrete spectra by plotting in Fig. 4 the effective oscillator strength distributions of the $4d \rightarrow 5f, 6f, \dots \ ^1P$ transitions for Xe- Nd^{6+} as functions of photon energy. The resonant nature of partial orbital collapse is unmistakable. In fact, the resulting spectrum actually resembles the photoionization cross section of neutral Xe, as both of them are due to the interaction of the $nf, \epsilon f$ wave functions with the inner well resonance. We note that the $4f \ ^1P$ lines are omitted in Fig. 4 because their behaviors are different from those of higher $nf \ ^1P$ lines. In particular, the latter ones disappear quickly with increasing Z , while the former ones remain strong after orbital collapse.

The interpretation of the Ba^{2+} spectrum is now very simple. In Fig. 5, we show the experimental and theoretical Ba^{2+} spectrum along with the quantum defects of the 1P channel. According to potential scattering theory,¹⁷ the width of a resonance is determined by the rate of increase of μ (the slope of the phase shift curve at the center of the resonance) and its center is located at a point where μ increases by one-half. The latter condition is approxi-

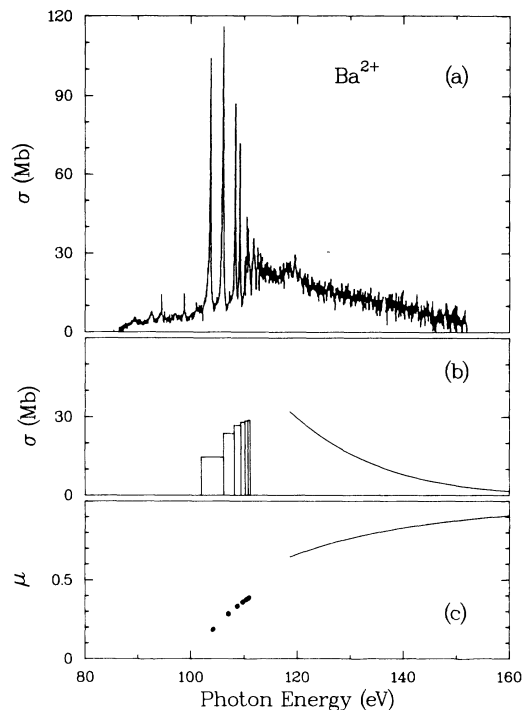


FIG. 5. Comparison between experimental and theoretical Ba^{2+} spectra. (a) Experimental absorption spectrum of Lucatoro *et al.*, Ref. 7; (b) theoretical absorption spectrum as shown in Fig. 2; (c) quantum-defect functions for Ba^{2+} as shown in Fig. 3.

mately satisfied at $\mu=0.5$, as μ starts from a very small value (or equivalently, μ reaches a value of about 1) for Xe-like ions. Thus the quantum defects shown in Fig. 5(c) not only demonstrate the presence of the inner well resonance, but also show that this resonance is very close to the $4d$ threshold in Ba^{2+} , with a very broad width of over 50 eV. As a result, the inner well resonance interacts with and affects both the continuum immediately above it and the entire Rydberg series below it. This gives rise to the large cross section at the onset of photoionization, and strong resonance lines in the observed Ba^{2+} spectrum. The profile of this inner well resonance is clearly seen in the theoretical absorption spectrum.

In Fig. 5, the agreement between experimental and theoretical Ba^{2+} spectra is in fact quite good, except for the profiles of the resonance lines. Nevertheless, the comparison clearly identifies the observed lines as the $4d \rightarrow nf \ ^1P$ transitions, with $n=4,5,6$, etc. Also, the areas under these lines are comparable to those under corresponding rectangles. Thus if the experimental resolution is very poor, these sharp lines will be averaged out, resulting in an observed spectrum that should be much closer to the theoretical one.

From these discussions, it is also clear that the $4f \ ^1P$ level is always the lowest level in the $nf \ ^1P$ series and is never pushed into the continuum by the exchange interaction, regardless of how strong it may be. However, in a CI calculation involving basis functions, the identification of the $4f \ ^1P$ level can be a problem when the wave functions are strongly term dependent. In particular, if the $4f$ wave function in the basis set is collapsed while the one in

the $4f^1P$ state is not, such as in Ba and Ba^{2+} , the $4f$ basis function will resemble the inner well eigenfunction rather than the $4f^1P$ one. Thus in a CI calculation for the $4f^1P$ level one can actually end up with the inner well eigenstate, which can either be above or below the ionization threshold. This, in turn, leads to the model that discrete energy levels can be raised into the far continuum by orbital collapse.⁶

Even though the labeling of the $4f^1P$ state in CI calculations can be misleading, the model nevertheless is correct in interpreting the absorption peak in rare-earth spectra as due to excitation to this collapsed $4f$ state, followed by autoionization into the continuum. This, of course, is just another way of saying that the inner well resonance in the 1P channel is responsible for the observed spectra. In this respect, the discrepancy between Lucatoro *et al.*⁷ and Connerade and Mansfield⁸ on the location of the $4f^1P$ state in Ba^{2+} simply reflects the model dependence in finding the inner well resonance. From our discussion here, it is clear that the exact location of this resonance is not very crucial. As long as it is close to the ionization limit and has a very broad width, it will give rise to the observed Ba^{2+} spectrum.

IV. ORBITAL COLLAPSE ALONG ISOELECTRONIC SEQUENCES

To complete our discussion, we should note that because we are interested in the collapse phenomenon along an isoelectronic sequence, there are slight differences between the usual discussions of orbital collapse and the present one. To clarify this point, we compare, in Figs. 6 and 7, the systematic changes in the effective potentials of f electrons for Xe, Cs, Ba, and La with those for Xe, Cs^+ , Ba^{2+} , and La^{3+} , respectively. The effective potentials are

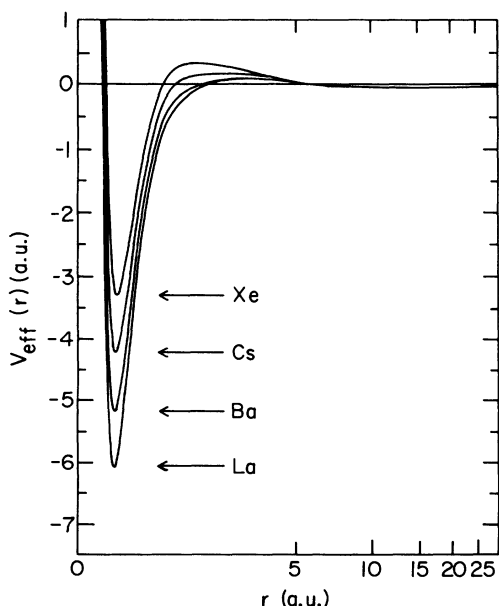


FIG. 6. Effective potential $V_{\text{eff}}(r)$ of f electrons for Xe, Cs, Ba, and La.

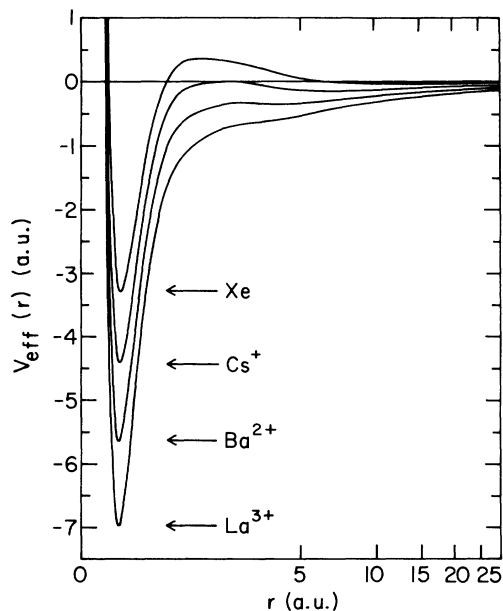


FIG. 7. Effective potential $V_{\text{eff}}(r)$ of f electrons for Xe, Cs^+ , Ba^{2+} , and La^{3+} .

obtained from a Hartree-Slater (HS) calculation.¹⁸ Since we are interested in qualitative features only, for brevity, all subsequent discussions will be based on configuration-average results unless otherwise specified.

As one can see in Figs. 6 and 7, the inner well deepens with increasing Z in both cases, and in fact with a comparable rate. As a result, the (configuration-average) $4f$ orbital is collapsed in neutral Ba as well as in Ba^{2+} . However, as $V_{\text{eff}}(r) \rightarrow -Z_c/r$ for large r , the outer well remains very constant along the neutral sequence ($Z_c = 1$), while it also deepens with increasing Z along the isoelectronic sequence ($Z_c = 1-4$). More importantly, the potential barrier is reduced only slightly for neutral atoms in going along the periodic table, while it disappears quickly along the isoelectronic sequence. As a result, regardless of whether the $4f$ orbital is collapsed or not, higher nf orbitals of the neutral atoms are restricted by the potential barrier to reside in the outer well, while those of the stripped ions are no longer prevented physically from entering the inner region, though as eigenfunctions of the potential, they reside in the outer region. At the same time, there should be steady contractions of nf wave functions due to the increased effective nuclear charge.

Along the periodic table, since the outer well remains very shallow, the eigenstate of the inner well can sink below the nf series very quickly. This leads to the sudden decrease in energy and size of the $4f$ orbital and hence the name "collapse." Along isoelectronic sequences, however, the sinking of the inner well eigenstate is now competing with the lowering of the outer well with increasing Z , and the process takes place over several ions. This leads to partial orbital collapse as discussed earlier. Because of the more gradual decrease in energy and size of the $4f$ orbital, the name collapse is actually not very appropriate, but we still use it to distinguish the change to the $4f$ wave function when it becomes the eigenfunction of the inner well,

as opposed to its natural contraction with increasing Z .

From Fig. 7, it is obvious that the potential barrier between the inner and outer wells disappears quickly along the isoelectronic sequence. As a result, the outer region of the effective potential no longer forms a well, and the name "outer well" is not very appropriate. However, as the collapse phenomenon depends mainly on the existence of eigenstates in the inner well, an actual positive potential barrier is not important. For convenience, we shall continue to use the name outer well to represent the outer hydrogenic region of the effective potential. It is interesting to note that if there is a strong potential barrier, the tunneling effect between the two wells will be suppressed, and it will be very difficult to find a wave function with substantial amplitude in both wells. This leads to the suggestion that the transfer of the wave function from the outer to the inner well should always occur abruptly.¹⁹ In reality, when the potential barrier is poorly defined, as in the present case, wave functions can be hybridized, and partial orbital collapse can occur over several stages of ionization.³ This, of course, is crucial to the interpretation of the Ba^{2+} spectrum here.

To show the effect of orbital collapse on nf wave functions, we first note that away from the range of Z where the $4f$ orbital is collapsing, these nf wave functions are determined mainly by the outer well, and are only weakly

perturbed by the inner well. Since the outer well is dominated by the long-range Coulomb potential, they are hydrogenlike, with very small quantum defects ($\nu \simeq n$). A consequence of orbital collapse is the appearance of an additional nonhydrogenic state (the lowest eigenstate of the inner well) below the entire nf series. This is most obvious if we compare the ν 's of the nf levels for $Z=54$ with those for $Z=60$ in Fig. 1. It is obvious that the two series are basically the same, with ν nearly an integer for all but the lowest $n=4$ levels of Nd^{6+} . However, since we always label the lowest nf state as the $4f$, what we call $4f, 5f, \dots$ states in Xe actually become $5f, 6f, \dots$ states, respectively, in Nd^{6+} . In other words, after $4f$ orbital collapse takes place, the nf wave functions should look like the hydrogenic $(n-1)f$ wave functions for $n \geq 5$. This, of course, is consistent with the fact that the effective quantum numbers have to decrease by 1 so that $\nu \simeq n-1$ rather than $\nu \simeq n$. The only exception is the $4f$ level whose ν decreases by more than 1, since it no longer is an eigenstate of the outer well after its collapse.

The situation is clearly shown in Figs. 8 and 9, where we plot the (configuration-average) HF $4f$ and $5f$ wave functions for Xe, Cs, Ba, and La and for Xe, Cs^+ , Ba^{2+} , and La^{3+} , respectively. Hydrogenic $4f$ and $5f$ wave functions are also shown for comparison purposes. As one can see in these figures, the $4f$ and $5f$ wave functions of Xe

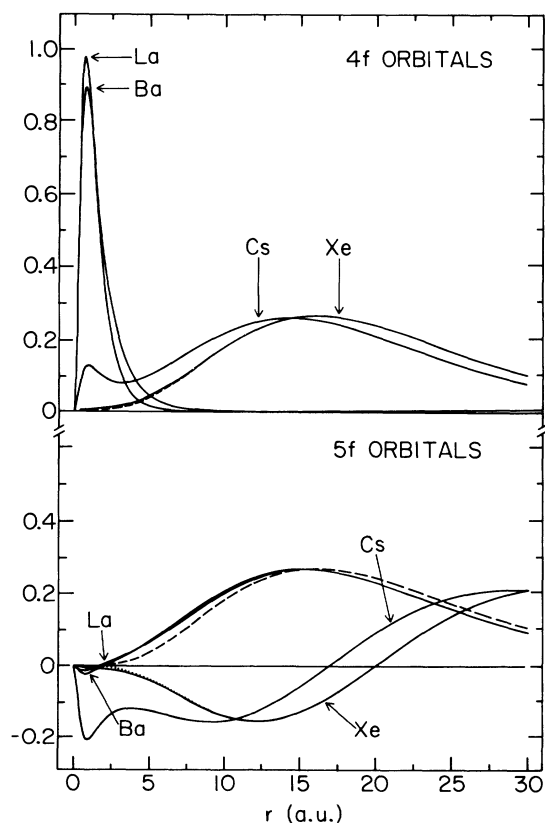


FIG. 8. Configuration-average $4f$ and $5f$ wave functions for Xe, Cs, Ba, and La. Dashed and dotted curves are hydrogenic $4f$ and $5f$ wave functions with $Z=1$, respectively. These hydrogenic wave functions are almost the same as the corresponding Xe wave functions.

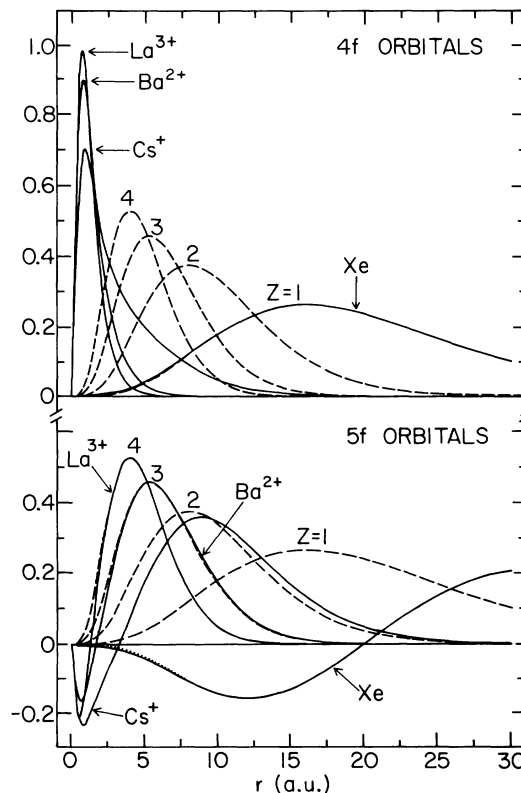


FIG. 9. Configuration-average $4f$ and $5f$ wave functions for Xe, Cs^+ , Ba^{2+} , and La^{3+} . Dashed curves are hydrogenic $4f$ wave functions with $Z=1, 2, 3,$ and 4 . Dotted curve is the hydrogenic $5f$ wave function with $Z=1$. Hydrogenic $4f$ and $5f$ wave functions with $Z=1$ are almost the same as the corresponding Xe wave functions.

are almost identical to the hydrogenic $4f$ and $5f$ ones. After the collapse, the $4f$ wave functions of Ba, La, Ba^{2+} , and La^{3+} no longer resemble hydrogenic $4f$ wave functions, but their $5f$ wave functions clearly resemble hydrogenic $4f$ wave functions in the outer region. As for the hybrid wave functions of Cs and Cs^+ , they are at a stage where the eigenstate of the inner well is interacting strongly with those of the outer one. Thus they have sizeable amplitudes in both wells, and look quite different from other wave functions.

One also notices in Fig. 8 that there are sudden changes in the nf ($n=5$) wave functions from Xe to Ba because of the orbital collapse, and that the wave functions of Ba and La are quite similar because they should resemble corresponding hydrogenic $(n-1)f$ ($4f$ in Fig. 8) wave functions with $Z=1$. Thus even though the $4d \rightarrow 4f$ transition is enhanced by the $4f$ orbital collapse, $4d \rightarrow nf$ transitions with $n \geq 5$ remain suppressed by the potential barrier. On the other hand, along the isoelectronic sequence, there are steady contractions of the nf wave functions as shown in Fig. 9 in spite of the sudden change in the wave functions in going from Xe to Ba^{2+} . As a result, $4d \rightarrow nf$ transitions for stripped ions are no longer suppressed even for higher nf states. However, once the $4f$ orbital is collapsed and resides in the inner well, the amplitudes of higher nf orbitals in the inner region will again be suppressed because of the orthonormality requirement among nf wave functions and the eigenfunction properties. This is reflected in the rapid decrease in the absorption oscillator strengths for $4d \rightarrow 5f, 6f, \dots$ 1P transitions in higher Z ions as shown in Table I.

Finally, we should mention that there are two equivalent ways of describing the sudden changes in the nf wave functions from $Z=54$ to $Z=56$. If one treats the interaction with the inner well as a perturbation [more precisely, treats $\Delta V = V_{\text{eff}}(r) + Z_c/r$ as a perturbation], then the unperturbed nf eigenfunctions of the outer well should pick up an extra node in the inner region as a result of orbital collapse. Another way of putting it is that when the inner well is deep enough, it forces the nf wave functions to oscillate once in the inner region so that orthonormality with the collapsed $4f$ orbital is retained. Thus in the outer region where these wave functions peak, they still look like hydrogenic nf wave functions, but because of the extra node in the inner region, they are classified as $(n+1)f$ wave functions. Similar observation was made by Wendin and Starace²⁰ in a different situation. They showed that when additional correlation from a term-dependent HF calculation is used as perturbations in a configuration-average HF calculation, the $4f$ orbitals for Ba and La shown in Fig. 8 are so strongly mixed with the nf orbitals with $n > 4$ that the latter all lose their inner nodes. Thus the configuration-average nf orbitals become essentially the term-dependent $(n-1)f$ orbitals. This, of course, is due to the fact that the $4f$ orbitals for Ba and

La are collapsed in a configuration-average HF calculation but are not collapsed in a term-dependent HF calculation.

Adiabatically, if we "tune" the nuclear charge continuously, the amplitudes of the nf wave functions in the inner region will be enhanced when the eigenstate of the inner well passes through the nf levels of the outer well. This is what happens to the wave functions of Cs and Cs^+ in Figs. 8 and 9. After the inner well eigenstate sinks below the entire Rydberg series, the $4f$ wave function remains nodeless but higher nf ones will have their first nodes shifted from the outer well into the inner one. At the same time, there are step decreases of one in the effective quantum numbers. As a result, higher nf wave functions actually look like hydrogenic $(n-1)f$ ones. An example of this change is given by Band *et al.*¹⁵ for the $5f$ wave function of the $6s^2nf$ configuration for $Z=56$ to 57 . Regardless of which approach one takes, the fact remains that the collapse of the $4f$ orbital leads to the appearance of a node in the nf wave function ($n \geq 5$) in the inner region, and the relabeling of the Rydberg series.

V. CONCLUSION

In this work, we reexamine the collapse phenomenon based on Goepfert Mayer's model.¹ We find that the collapse of the $4f$ orbital for Xe-like ions is strongly term dependent. In particular, for Ba^{2+} the $4f$ orbital is collapsed in the $4d^9 4f^3 P$ and 3D states but is only partially collapsed in the 1P state. The partial collapse of the $4f$ orbital in the 1P channel is responsible for the observed Ba^{2+} spectrum. The effect of full orbital collapse will not show up in Xe-like ions until $Z \geq 58$. Along with the RRPA results of Cheng and Johnson,¹³ we further show that orbital collapse and partial orbital collapse are basically shape resonance effects arising from the interaction between the inner well eigenstate and the $nf, \epsilon f$ states. Finally, while our discussions are mainly qualitative in nature, we expect the dominant features of the spectra and the collapse phenomenon described here to be reliable. Nevertheless, a more quantitative study of the spectra of Xe-like ions is still desirable, possibly one using relativistic many-body techniques such as the multiconfiguration Dirac-Fock method.

Note added. After the submission of this paper, we learned that there are two recent papers by Connerade,²¹ whose interpretation of the $4d$ spectra of Ba, Ba^+ , and Ba^{2+} is very similar to ours.

ACKNOWLEDGMENTS

This work is performed in part under the auspices of the U.S. Department of Energy, Office of Basic Energy Sciences, under Contract No. W-31-109-ENG-38 and Contract No. DE-AS05-80-ER10618.

¹M. Goepfert Mayer, Phys. Rev. **60**, 184 (1941).

²J. P. Connerade, Contemp. Phys. **19**, 415 (1978).

³R. I. Karaziya, Usp. Fiz. Nauk **135**, 79 (1981) [Sov. Phys.—

Usp. **24**, 775 (1981)].

⁴T. B. Lucatoro, T. J. McIlrath, W. T. Hill, and C. W. Clark, in *Proceedings of the International Conference on X-Ray and*

- Atomic Inner-Shell Physics, Eugene, Oregon, 1982, AIP Conference Proceedings No. 94, 1982*, edited by B. Crasemann (AIP, New York, 1982).
- ⁵J. W. Cooper, Phys. Rev. Lett. **13**, 762 (1964).
- ⁶J. L. Dehmer, A. F. Starace, U. Fano, J. Sugar, and J. W. Cooper, Phys. Rev. Lett. **26**, 1521 (1971).
- ⁷T. B. Lucatorto, T. J. McIlrath, J. Sugar, and S. M. Younger, Phys. Rev. Lett. **47**, 1124 (1981).
- ⁸J. P. Connerade and M. W. D. Mansfield, Phys. Rev. Lett. **48**, 131 (1982).
- ⁹In Ref. 8, the energy of the $4d^9 4f^1 P$ state of Ba^{2+} is given by 118.4 eV (104.7 Å), and is higher than the experimental $^2D_{5/2}$ and $^2D_{3/2}$ threshold energies of 114.7 and 117.2 eV, respectively, given in Ref. 7.
- ¹⁰K. Nuroh, M. J. Stott, and E. Zaremba, Phys. Rev. Lett. **49**, 862 (1982).
- ¹¹C. Froese Fischer, *The Hartree-Fock Methods for Atoms: A Numerical Approach* (Wiley, New York, 1977).
- ¹²S. T. Manson and J. W. Cooper, Phys. Rev. **165**, 126 (1968).
- ¹³K. T. Cheng and W. R. Johnson, Phys. Rev. A **28**, 2820 (1983), following paper.
- ¹⁴M. J. Seaton, J. Phys. B **11**, 4067 (1978); U. Fano, J. Opt. Soc. Am. **65**, 979 (1975).
- ¹⁵I. M. Band, V. I. Fomichev, and M. B. Trzhaskovskaya, J. Phys. B **14**, 1103 (1981).
- ¹⁶J. E. Hansen, A. W. Fliflet, and H. P. Kelly, J. Phys. B **8**, L127 (1975).
- ¹⁷G. Baym, *Lectures on Quantum Mechanics* (Benjamin, Reading, Mass., 1969), Chap. 9.
- ¹⁸J. P. Desclaux, Comput. Phys. Commun. **1**, 216 (1969).
- ¹⁹D. C. Griffin, K. L. Andrew, and R. D. Cowan, Phys. Rev. **177**, 62 (1969).
- ²⁰G. Wendin and A. F. Starace, J. Phys. B **11**, 4119 (1978).
- ²¹J. P. Connerade, J. Phys. B **15**, L881 (1982); **16**, L257 (1983).